A Sliding Mode Control for Dual-Stator Induction Motor Drives Fed by Matrix Converters

H. Amimeur, R. Abdessemed, D. Aouzellag, K. Ghedamsi, F. Hamoudi and S. Chekkal

***Abstract*— In this paper, a sliding mode control strategy (SMC) associated to the field-oriented control (FOC) of dual-stator induction motor drives (DSIM) fed by matrix converters (MC) is investigated. The induction machine has two sets of stator three-phase windings spatially shifted by 30 electrical degrees; the sliding mode control is a robust non linear algorithm which uses discontinuous control to force the system states trajectories to join some specified sliding surface, it has been widely used for its robustness to model parameter uncertainties and external disturbances, is studied. Is also investigated the direct AC/AC frequency converter, called matrix converter. In order to verify the validity of the proposed method, a dynamic model of the proposed system has been simulated, to demonstrate the performance of the system.**

***Index Terms*— Dual-stator induction motor drives, field-oriented control, matrix converter, sliding mode control.**

I. Introduction

INVENTED by Nikola Tesla in 1888, the alternating-current (AC) induction motor has had a major role in the development of the electrical industry [1]. The primary advantages of induction machine are less maintenance cost, brushless construction (squirrel-cage rotor), better transient, etc.

Since the late 1920s, dual-stator AC machines have been used in many applications (such as: pumps, fans, compressors, rolling mills, cement mills, mine hoists [2]), for their advantages in power segmentation, reliability, lower torque pulsations, less dc-link current harmonics, reduced rotor harmonics and higher power per ampere ratio for the same machine volume, etc. [3]-[6].

Matrix converter (MC) is a modern energy conversion device that has been developed over the last two decades [7]. The matrix converter drive has recently attracted industrial applications and the technical development has been further accelerated because of the increasing importance of power quality and energy efficiency [8]. Furthermore, matrix converter (MC) eliminates the dc-link filter elements and thus resolves the size, weight and reliability issues and also provides an option for the design of the converter as a compact/modular unit. The main advantages of the MC allows for power factor correction (including unity), bidirectional power flow and the possibility for more compact equipment building [9]-[12]. The VENTURINI classical algorithm for control of the MC is used [13].

H. Amimeur, R. Abdessemed and F. Hamoudi are with the group LEB-Research Laboratory, Department of Electrical Engineering, University of Batna. Street Chahid Mohamed El hadi Boukhlouf, 05000, Batna, Algeria (e-mail: amimeurhocine2002@yahoo.fr; r.abdessemed@lycos.com; f_hamoudi@yahoo.fr).

D. Aouzellag, K. Ghedamsi and S. Chekkal are with Electrical Engineering Department, A. Mira University, Bejaia, Algeria (e-mail: aouzellag@hotmail.com; kghedamsi@yahoo.fr).

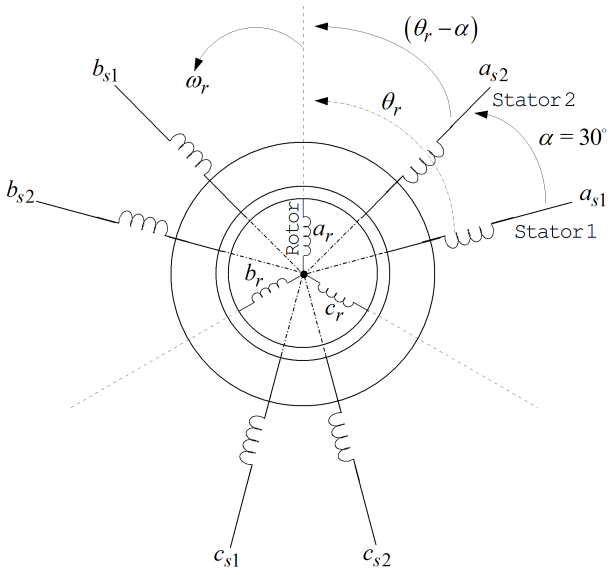

Fig. 1. Scheme of dual-stator windings induction machine.

The sliding mode control theory was proposed by Utkin in 1977 [14]. Thereafter, the theoretical works and its applications of the sliding mode controller were developed. Since the robustness is the best advantage of a sliding mode control, it has been widely employed to control nonlinear systems, especially the systems that have model uncertainty and external disturbance [15]-[19]. These advantages justify the necessity of applying this kind of control for the DSIM.

The paper is organized as follows. Description of the DSIM and the mathematical model are provides in Section II. The field oriented control of a DSIM is developed in Section III. The sliding mode control theory is presented in Section IV. The sliding mode control of a DSIM is developed in Section V and its proprieties are validated through simulation results in Section VII. The matrix converter modeling is presented in Section VI. Finally, Section VIII summarizes conclusions.

II. Machine Model

A schematic of the stator and rotor windings for a dual-stator induction machine is given in Fig. 1. The six stator phases are divided into two wye-connected three-phase sets, labeled (a_{s1}, b_{s1}, c_{s1}) and (a_{s2}, b_{s2}, c_{s2}), whose magnetic axes are displaced by $\alpha = 30°$ electrical angle. The windings of each three-phase set are uniformly distributed and have axes

that are displaced 120° apart. The three-phase rotor windings (a_r, b_r, c_r) are also sinusoidally distributed and have axes that are displaced by 120° apart [20]-[22].

The following assumptions have been made in deriving the dual-stator induction machine model:

- Machine windings are sinusoidally distributed;
- The two stators have same parameters;
- Flux path is linear;
- The magnetic saturation and the mutual leakage are neglected.

The electrical equations of the dual-stator induction motor drives in the synchronous reference frame $(d-q)$ are this given by [23]-[25]

$$v_{d1} = r_1 \imath_{d1} + p\psi_{d1} - \omega_e \psi_{q1} \quad (1)$$
$$v_{q1} = r_1 \imath_{q1} + p\psi_{q1} + \omega_e \psi_{d1} \quad (2)$$
$$v_{d2} = r_2 \imath_{d2} + p\psi_{d2} - \omega_e \psi_{q2} \quad (3)$$
$$v_{q2} = r_2 \imath_{q2} + p\psi_{q2} + \omega_e \psi_{d2} \quad (4)$$
$$v_{dr} = r_r \imath_{dr} + p\psi_{dr} - (\omega_e - \omega_r)\psi_{qr} = 0 \quad (5)$$
$$v_{qr} = r_r \imath_{qr} + p\psi_{qr} + (\omega_e - \omega_r)\psi_{dr} = 0 \quad (6)$$

with,
v_{d1}, v_{d2}, $\imath_{d1}$, $\imath_{d2}$, and ψ_{d1}, ψ_{d2} are respectively the "d" components of the stator voltages, currents and flux linkage;
v_{q1}, v_{q2}, $\imath_{q1}$, $\imath_{q2}$, and ψ_{q1}, ψ_{q2} are respectively the "q" components of the stator voltages, currents and flux linkage;
v_{dr}, $\imath_{dr}$ and ψ_{dr} are respectively the "d" components of the rotor voltage, current and flux linkage;
v_{qr}, $\imath_{qr}$ and ψ_{qr} are respectively the "q" components of the rotor voltage, current and flux linkage;
r_1, r_2 and r_r are respectively the per phase stator resistance and the per phase rotor resistance;
ω_e is the speed of the synchronous reference frame;
ω_r is the rotor electrical angular speed;
p is the derivative operator.

The expressions for stator and rotor flux linkages are

$$\psi_{d1} = L_1 \imath_{d1} + L_m(\imath_{d1} + \imath_{d2} + \imath_{dr}) \quad (7)$$
$$\psi_{q1} = L_1 \imath_{q1} + L_m(\imath_{q1} + \imath_{q2} + \imath_{qr}) \quad (8)$$
$$\psi_{d2} = L_2 \imath_{d2} + L_m(\imath_{d1} + \imath_{d2} + \imath_{dr}) \quad (9)$$
$$\psi_{q2} = L_2 \imath_{q2} + L_m(\imath_{q1} + \imath_{q2} + \imath_{qr}) \quad (10)$$
$$\psi_{dr} = L_r \imath_{dr} + L_m(\imath_{d1} + \imath_{d2} + \imath_{dr}) \quad (11)$$
$$\psi_{qr} = L_r \imath_{qr} + L_m(\imath_{q1} + \imath_{q2} + \imath_{qr}) \quad (12)$$

where,
L_1, L_2 and L_r are respectively the per phase stator self inductance and the per phase rotor self inductance;
L_m is the mutual inductance between stator and rotor.

The electromagnetic torque is evaluated as

$$T_{em} = P\frac{L_m}{L_m + L_r}\left[(\imath_{q1} + \imath_{q2})\psi_{dr} - (\imath_{d1} + \imath_{d2})\psi_{qr}\right] \quad (13)$$

with, P is the number of pole pairs.

The mechanical equation of machine is described as

$$Jp\Omega + f\Omega = T_{em} - T_L \quad (14)$$

III. Field Oriented Control of a DSIM

The main objective of the vector control of induction motors is, as in DC machines, to independently control the torque and the flux [26]. In this order, we propose to study the FOC of the DSIM. The control strategy used consists to maintain the quadrate component of the flux null $(\psi_{qr} = 0)$ and the direct flux equals to the reference $(\psi_{dr} = \psi_r^*)$:

$$\psi_{dr} = \psi_r^* \quad (15)$$
$$\psi_{qr} = 0 \quad (16)$$
$$p\psi_r^* = 0 \quad (17)$$

Substituting (15), (16) and (17) into (5) and (6), yields

$$r_r \imath_{dr} + p\psi_r^* = 0 \Rightarrow \imath_{dr} = 0 \quad (18)$$
$$r_r \imath_{qr} + \omega_{sl}^* \psi_r^* = 0 \Rightarrow \imath_{qr} = -\frac{\omega_{sl}^* \psi_r^*}{r_r} \quad (19)$$

with, $\omega_{sl}^* = \omega_e^* - \omega_r$, ($\omega_{sl}$ is the slip speed).

The rotor currents in terms of the stator currents are divided from (11) and (12) as

$$\imath_{dr} = \frac{1}{L_m + L_r}\left[\psi_r^* - L_m(\imath_{d1} + \imath_{d2})\right] \quad (20)$$
$$\imath_{qr} = -\frac{L_m}{L_m + L_r}(\imath_{q1} + \imath_{q2}) \quad (21)$$

Substituting (21) into (19), obtain

$$\omega_{sl}^* = \frac{r_r L_m}{(L_m + L_r)}\frac{(\imath_{q1} + \imath_{q2})}{\psi_r^*} \quad (22)$$

The final expression of the electromagnetic torque is

$$T_{em}^* = \frac{PL_m}{(L_m + L_r)}(\imath_{q1} + \imath_{q2})\psi_r^* \quad (23)$$

With taking into the rotor field orientation, the stator voltage equations (1)–(4) can be rewritten as

$$v_{d1}^* = r_1 \imath_{d1} + L_1 p\imath_{d1} - \omega_e^*(L_1 \imath_{q1} + \tau_r \psi_r^* \omega_{sl}^*) \quad (24)$$
$$v_{q1}^* = r_1 \imath_{q1} + L_1 p\imath_{q1} + \omega_e^*(L_1 \imath_{d1} + \psi_r^*) \quad (25)$$
$$v_{d2}^* = r_2 \imath_{d2} + L_2 p\imath_{d2} - \omega_e^*(L_2 \imath_{q2} + \tau_r \psi_r^* \omega_{sl}^*) \quad (26)$$
$$v_{q2}^* = r_2 \imath_{q2} + L_2 p\imath_{q2} + \omega_e^*(L_2 \imath_{d2} + \psi_r^*) \quad (27)$$

where, $\tau_r = \frac{L_r}{r_r}$ is time rotor constant.

Consequently, the electrical and mechanical equations for the system after these transformations in the space control may be written as follows:

$$p\imath_{d1} = \frac{1}{L_1}\left\{v_{d1}^* - r_1 \imath_{d1} + \omega_e^*(L_1 \imath_{q1} + \tau_r \psi_r^* \omega_{sl}^*)\right\} \quad (28)$$
$$p\imath_{q1} = \frac{1}{L_1}\left\{v_{q1}^* - r_1 \imath_{q1} - \omega_e^*(L_1 \imath_{d1} + \psi_r^*)\right\} \quad (29)$$
$$p\imath_{d2} = \frac{1}{L_2}\left\{v_{d2}^* - r_2 \imath_{d2} + \omega_e^*(L_2 \imath_{q2} + \tau_r \psi_r^* \omega_{sl}^*)\right\} \quad (30)$$
$$p\imath_{q2} = \frac{1}{L_2}\left\{v_{q2}^* - r_2 \imath_{q2} - \omega_e^*(L_2 \imath_{d2} + \psi_r^*)\right\} \quad (31)$$
$$p\psi_r = -\frac{r_r}{L_r + L_m}\psi_r + \frac{r_r L_m}{L_r + L_m}(\imath_{d1} + \imath_{d2}) \quad (32)$$
$$p\Omega = \frac{1}{J}\left\{P\frac{L_m}{L_r + L_m}(\imath_{q1} + \imath_{q2})\psi_r^* - T_L - f\Omega\right\} \quad (33)$$

IV. Sliding Mode Control

We consider a system described by the following state space equation:

$$[\dot{X}] = [A][X] + [B][U] \tag{34}$$

with,
$[X] \in \mathbb{R}^n$ is the state vector;
$[U] \in \mathbb{R}^m$ is the control input vector;
$[A]$ and $[B]$ are system parameter matrices.

The first phase of the control design consists of choosing the number of the switching surfaces $S(x)$. Generally this number is equal the dimension of the control vector U. In order to ensure to convergence of the state variable x to its reference value x^*, [16] proposes a general function of the switching surface:

$$S(x) = (\frac{d}{dt} + \lambda)^{r-1} e(x) \tag{35}$$

where,
λ is a strictly positive constant;
r is the smallest positive integer such that $\frac{\partial \dot{S}}{\partial U} \neq 0$: ensure controllability;
$e(x) = x^* - x$ is the error variable.

The second phase consists to find the control law which meets the sufficiency conditions for the existence and reachibility of a sliding mode such as [14], [27]

$$S(x)\dot{S}(x) < 0 \tag{36}$$

Intuitively, the existence of a sliding mode on the sliding surface implies stability of the system. One of the possible solutions is given by

$$U_c = U_{eq} + U_n \tag{37}$$

U_{eq} is the so called equivalent control. It plays the feedback linearization role is the solution of

$$\dot{S}(x) = 0 \Leftrightarrow \frac{\partial S}{\partial X}\{[A][X] + [B]U_{eq}\} + \frac{\partial S}{\partial X}[B]U_n = 0 \tag{38}$$

During the sliding mode, the U_n is equal zero, then U_{eq} is

$$U_{eq} = -\left\{\frac{\partial S}{\partial X}[B]\right\}^{-1}\left\{\frac{\partial S}{\partial X}[A][X]\right\} \tag{39}$$

with

$$\frac{\partial S}{\partial X}[B] \neq 0 \tag{40}$$

During the convergence mode, the $U_n \neq 0$. We substituting (39) into (38) yields

$$\dot{S}(x) = \frac{\partial S}{\partial X}[B]U_n \tag{41}$$

Substituting (41) into (36), obtain

$$S(x)\frac{\partial S}{\partial X}[B]U_n < 0 \tag{42}$$

So that the state trajectory be attracted to the switching surface $S(x) = 0$. A commonly used from of U_n is a constant relay control [27].

$$U_n = k_x sgn(S(x)) \tag{43}$$

$sgn(S(x))$ is a sign function, which is defined as

$$sgn(S(x)) = \begin{cases} -1 & \text{if} \quad S(x) < 0 \\ 1 & \text{if} \quad S(x) > 0 \end{cases} \tag{44}$$

k_x is a constant.

This introduces some undesirable chattering. Hence, we will substitute it by the function plotted in Fig. 2.
Consequently, U_n is defined as

$$U_n = k_x \frac{S(x)}{|S(x)| + \xi_x} \tag{45}$$

ξ_x is small positive scalar.

V. Sliding Mode Control of a DSIM

The proposed control scheme is a cascade structure at it is shown in Fig. 3, in which six surfaces are required. The internal loops allow the control stator current components ($\imath_{d1}$, $\imath_{q1}$, $\imath_{d2}$ and $\imath_{q2}$), whereas the external loops provide the regulation of the speed Ω and the flux ψ_r. The bloc of the FOC(SMC) is presented in Fig. 4.

A. Design of the Switching Surfaces

In this work, six sliding surfaces are used and taken as follows since a first order is defined as

$$S(\Omega) = \Omega^* - \Omega \tag{46}$$

$$S(\psi_r) = \psi_r^* - \psi_r \tag{47}$$

$$S(\imath_{d1}) = \imath_{d1}^* - \imath_{d1} \tag{48}$$

$$S(\imath_{q1}) = \imath_{q1}^* - \imath_{q1} \tag{49}$$

$$S(\imath_{d2}) = \imath_{d2}^* - \imath_{d2} \tag{50}$$

$$S(\imath_{q2}) = \imath_{q2}^* - \imath_{q2} \tag{51}$$

B. Development of the Control Laws

By using the equations systems (28)-(33), (37) and (45), the regulators control laws are obtained as follows:

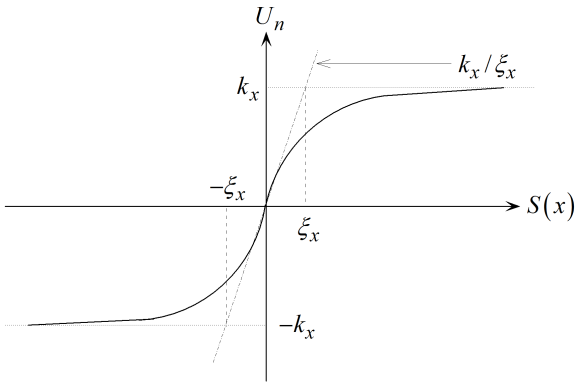

Fig. 2. Shape of the sgn function.

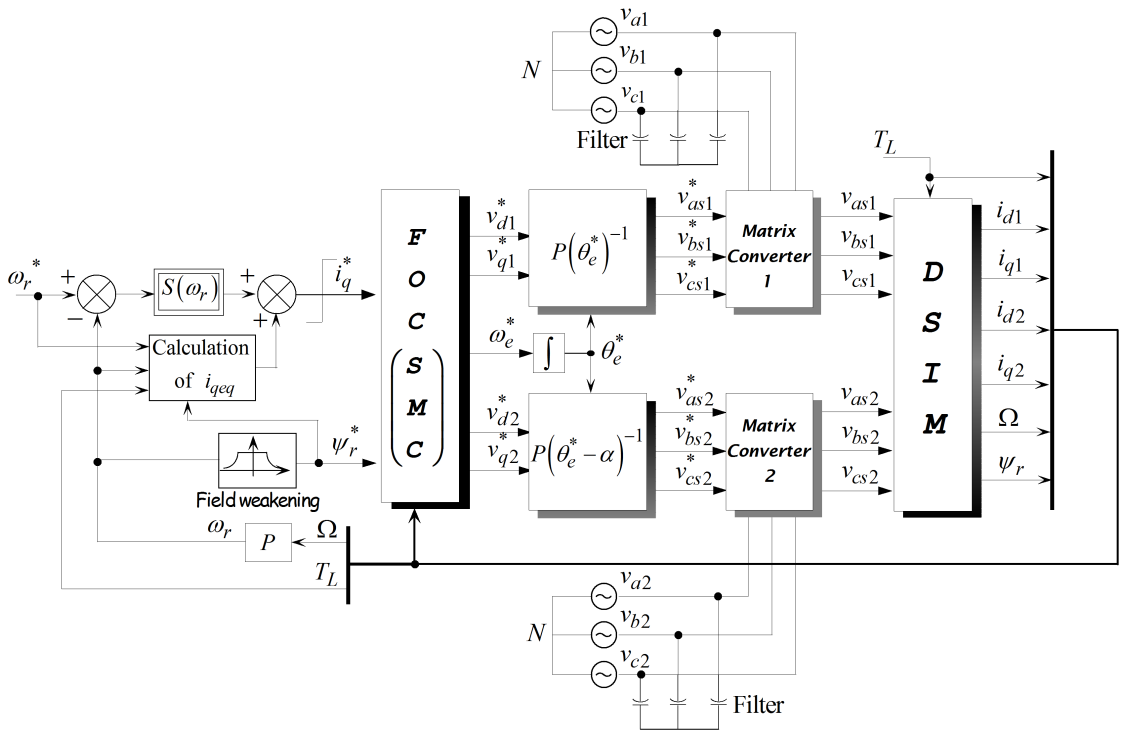

Fig. 3. Indirect FOC scheme for DSIM.

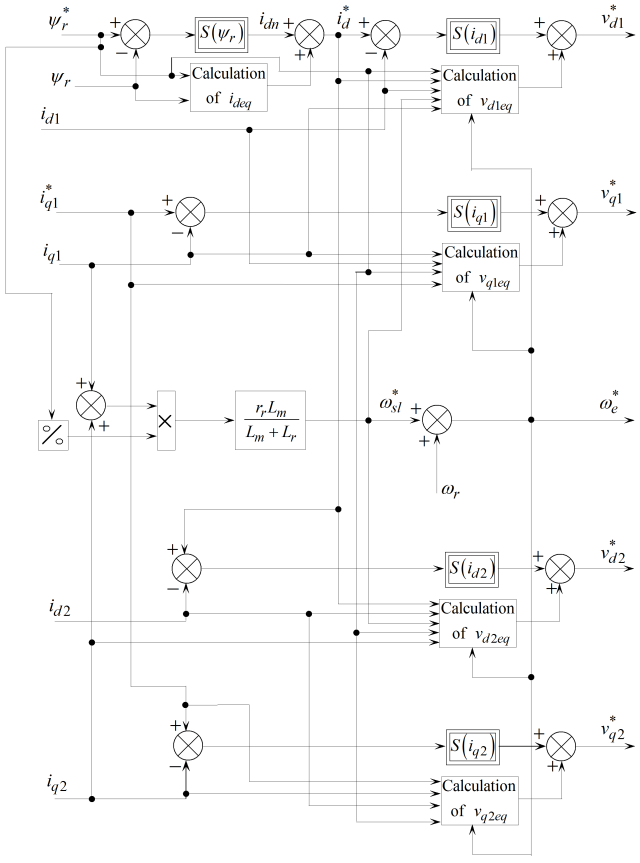

Fig. 4. Bloc diagram of the FOC (SMC).

1) For the Speed Regulator:

$$S(\omega_r)\dot{S}(\omega_r) < 0 \Rightarrow \imath_q^* = \imath_{qeq} + \imath_{qn} \tag{52}$$

with

$$\imath_q = \imath_{q1} + \imath_{q2} \quad \text{and} \quad \omega_r = P\Omega;$$

$$\imath_{qeq} = \frac{J}{P^2}\frac{L_r + L_m}{L_m \psi_r^*} + \left[p\omega_r^* \frac{f}{J}\omega_r + \frac{P}{J}T_L\right];$$

$$\imath_{qn} = k_{\omega_r}\frac{S(\omega_r)}{|S(\omega_r)| + \xi_{\omega_r}}.$$

2) For the Flux Regulator:

$$S(\psi_r)\dot{S}(\psi_r) < 0 \Rightarrow \imath_d^* = \imath_{deq} + \imath_{dn} \tag{53}$$

where

$$\imath_d = \imath_{d1} + \imath_{d2};$$

$$\imath_{deq} = \frac{L_r + L_m}{r_r L_m}\left[p\psi_r^* + \frac{r_r}{L_r + L_m}\psi_r\right];$$

$$\imath_{dn} = k_{\psi_r}\frac{S(\psi_r)}{|S(\psi_r)| + \xi_{\psi_r}}.$$

3) For the Stator Currents Regulators:

$$S(\imath_{d1})\dot{S}(\imath_{d1}) < 0 \Rightarrow v_{d1}^* = v_{d1eq} + v_{d1n} \tag{54}$$

$$S(\imath_{q1})\dot{S}(\imath_{q1}) < 0 \Rightarrow v_{q1}^* = v_{q1eq} + v_{q1n} \tag{55}$$

$$S(\imath_{d2})\dot{S}(\imath_{d2}) < 0 \Rightarrow v_{d2}^* = v_{d2eq} + v_{d2n} \tag{56}$$

$$S(\imath_{q2})\dot{S}(\imath_{q2}) < 0 \Rightarrow v_{q2}^* = v_{q2eq} + v_{q2n} \tag{57}$$

with

$$v_{d1eq} = L_1 i_{d1}^* + r_1 \imath_{d1} - \omega_e^* \left[L_1 \imath_{q1} + \tau_r \psi_r^* \omega_{sl}^* \right];$$
$$v_{q1eq} = L_1 i_{q1}^* + r_1 \imath_{q1} + \omega_e^* \left[L_1 \imath_{d1} + \psi_r^* \right];$$
$$v_{d2eq} = L_2 i_{d2}^* + r_2 \imath_{d2} - \omega_e^* \left[L_2 \imath_{q2} + \tau_r \psi_r^* \omega_{sl}^* \right];$$
$$v_{q2eq} = L_2 i_{q2}^* + r_2 \imath_{q2} + \omega_e^* \left[L_2 \imath_{d2} + \psi_r^* \right];$$

and

$$v_{d1n} = k_{d1} \frac{S(\imath_{d1})}{|S(\imath_{d1})| + \xi_{d1}};$$
$$v_{q1n} = k_{q1} \frac{S(\imath_{q1})}{|S(\imath_{q1})| + \xi_{q1}};$$
$$v_{d2n} = k_{d2} \frac{S(\imath_{d2})}{|S(\imath_{d2})| + \xi_{d2}};$$
$$v_{q2n} = k_{q2} \frac{S(\imath_{q2})}{|S(\imath_{q2})| + \xi_{q2}}.$$

To satisfy the stability condition of the system, the gains k_{ω_r}, k_{ψ_r}, k_{d1}, k_{q1}, k_{d2} and k_{q2} should be taken positive by selecting the appropriate values.

VI. Matrix Converter Modeling

Matrix converter consists of nine bidirectional switches, which are considered ideal for the ease of this presentation [28]. Each output phase is associated with three switches set connected to three input phases. This configuration of bidirectional switches enables the connection of any input phase a_1, b_1 or c_1 to any output phase A_1, B_1 or C_1 at any instant (matrix converter Fig. 3 and Fig. 5). The switching function of a switch S_{ij} in Fig. 3 is defined (referred to matrix converter 1) as

$$S_{ij} = \begin{cases} 1 & S_{ij} \text{ is closed,} \\ 0 & S_{ij} \text{ is open,} \end{cases} \tag{58}$$
$$i \in \{a_1, \quad b_1, \quad c_1\},$$
$$j \in \{A_1, \quad B_1, \quad C_1\}.$$

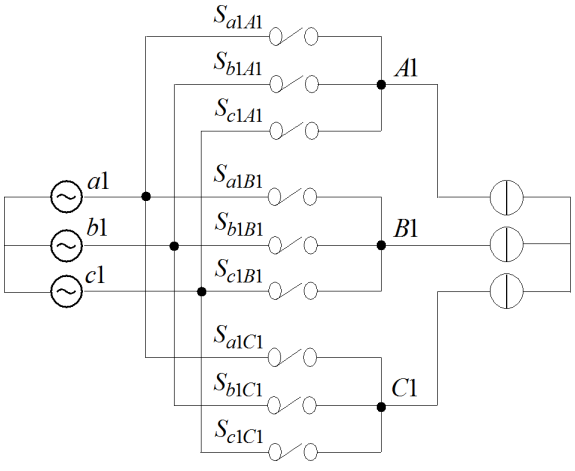

Fig. 5. Matrix converter topology.

A. The Switching Angles Formulation

The switching angles, of the nine-bidirectional switches S_{ij} which will be calculated, must comply with the following rules [7], [9].

1) At any time 't', only one switch S_{ij} ($j = 1, 2, 3$) will be in 'ON' state. This assures that no short circuit will occur at the input terminals;
2) At any time 't', at least two of the switches S_{ij} ($j = 1, 2, 3$) will be in 'ON' state. This condition guarantees a closed-loop path for the load current (usually this is an inductive current).

During the kth switching cycle T_s ($T_s = 1/f_s$) (Fig. 5), the first phase output voltage is given by

$$v_{a1} = \begin{cases} v_{A1} & \text{for} \quad 0 \le t - (k-1)T_s < m_{a1A1}^k T_s \\ v_{B1} & \text{for} \quad m_{a1A1}^k T_s \le t - (k-1)T_s < \\ & \qquad (m_{a1A1}^k + m_{a1B1}^k) T_s \\ v_{C1} & \text{for} \quad (m_{a1A1}^k + m_{a1B1}^k) T_s \le t - (k-1)T_s < T_s \end{cases} \tag{59}$$

where m_{ij}^k is defined by

$$m_{ij}^k = \frac{t_{ij}^k}{T_s} \tag{60}$$

where t_{ij}^k is the time interval when S_{ij} is in 'ON' state, during the kth cycle, and k being the switching cycle sequence number. The m_{ij}^k has the physical meaning of duty cycle. Also,

$$m_{iA1}^k + m_{iB1}^k + m_{iC1}^k = 0 \quad \text{and} \quad 0 < m_{ij}^k < 1$$

which means that during every cycle T_s, all switches of the first phase output voltages will turn on and off once (Fig. 6).

B. Algorithm of VENTURINI

The algorithm of VENTURINI [12], [13], allows a control of the S_{ij} switches so that the low frequency parts of the synthesized output voltages (v_{a1}, v_{b1} and v_{c1}) and the input currents (i_{A1r}, i_{B1r} and i_{C1r}) are purely sinusoidal with the prescribed values of the output frequency, the input frequency, the displacement factor and the input amplitude. The average values of the output voltages during the kth sequence are thus given by

$$\begin{aligned} v_{a1} &= \frac{t_{a1A1}^k}{T_s} v_{A1} + \frac{t_{a1B1}^k}{T_s} v_{B1} + \frac{t_{a1C1}^k}{T_s} v_{C1} \\ v_{b1} &= \frac{t_{b1A1}^k}{T_s} v_{A1} + \frac{t_{b1B1}^k}{T_s} v_{B1} + \frac{t_{b1C1}^k}{T_s} v_{C1} \\ v_{c1} &= \frac{t_{c1A1}^k}{T_s} v_{A1} + \frac{t_{c1B1}^k}{T_s} v_{B1} + \frac{t_{c1C1}^k}{T_s} v_{C1} \end{aligned} \tag{61}$$

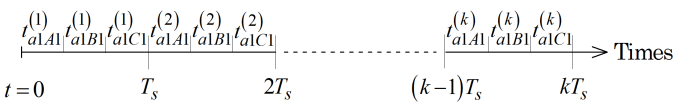

Fig. 6. Segmentation of the axis time for the consecutive orders of intervals closing of the switches.

If times of conduction are modulated in the shape of sinusoidal with the pulsation ω_m while T_s remains constant, such as $\omega_o = \omega_i + \omega_m$, these times are defined as follows:

1) For the 1^{st} phase, we have

$$\begin{aligned} t_{a1A1}&=\frac{T_s}{3}(1+2q\cos(\omega_m t+\theta)) \\ t_{a1B1}&=\frac{T_s}{3}(1+2q\cos(\omega_m t+\theta-\frac{2\pi}{3})) \\ t_{a1C1}&=\frac{T_s}{3}(1+2q\cos(\omega_m t+\theta-\frac{4\pi}{3})) \end{aligned} \quad (62)$$

2) For the 2^{nd} phase

$$\begin{aligned} t_{b1A1}&=\frac{T_s}{3}(1+2q\cos(\omega_m t+\theta-\frac{4\pi}{3})) \\ t_{b1B1}&=\frac{T_s}{3}(1+2q\cos(\omega_m t+\theta)) \\ t_{b1C1}&=\frac{T_s}{3}(1+2q\cos(\omega_m t+\theta-\frac{2\pi}{3})) \end{aligned} \quad (63)$$

3) For the 3^{rd} phase

$$\begin{aligned} t_{c1A1}&=\frac{T_s}{3}(1+2q\cos(\omega_m t+\theta-\frac{2\pi}{3})) \\ t_{c1B1}&=\frac{T_s}{3}(1+2q\cos(\omega_m t+\theta-\frac{4\pi}{3})) \\ t_{c1C1}&=\frac{T_s}{3}(1+2q\cos(\omega_m t+\theta)) \end{aligned} \quad (64)$$

where,
ω_i is the pulsation of the reference input current vector;
ω_o is the pulsation of the reference output voltage vector;
θ is the initial phase angle.

The output voltage is given by

$$\begin{bmatrix} v_{a1} \\ v_{b1} \\ v_{c1} \end{bmatrix} = \begin{bmatrix} 1+2q\cos\beta & 1+2q\cos\gamma & 1+2q\cos\delta \\ 1+2q\cos\delta & 1+2q\cos\beta & 1+2q\cos\gamma \\ 1+2q\cos\gamma & 1+2q\cos\delta & 1+2q\cos\beta \end{bmatrix} \times \begin{bmatrix} v_{A1} \\ v_{B1} \\ v_{C1} \end{bmatrix}$$

where

$$\begin{aligned} \beta&=\omega_m+\theta, \\ \gamma&=\beta-\frac{2\pi}{3}, \\ \delta&=\beta-\frac{4\pi}{3}, \\ \omega_m&=\omega_o+\omega_i. \end{aligned}$$

The running matrix converter with VENTURINI algorithm generates at the output a three-phase sinusoidal voltages system having in that order pulsation ω_m, a phase angle θ and amplitude qV_s ($0 < q < 0.866$ with modulation of the neutral) [13].

VII. Simulation Results and Discussion

The dual-stator induction motor parameters used in the simulation are given in the Appendix. The values of sliding mode switching gains are summarized by the table I below.

The first test concerns a no-load starting of the motor with a reference speed $n^* = 2500rpm$. Then a torque load $T_L = 14N.m$ is applied between $t = 1.5sec$ and $t = 2.5sec$. The results are shown in Fig. 7.

TABLE I
Sliding mode controller gains

$k_{\omega r}$	17.2	$\xi_{\omega r}$	0.95
$k_{\psi r}$	1.3	$\xi_{\psi r}$	0.01
$k_{d1} = k_{d2}$	185	$\xi_{d1} = \xi_{d2}$	0.1
$k_{q1} = k_{q2}$	200	$\xi_{q1} = \xi_{q2}$	0.12

The second test concerns a no-load starting of the motor with a reference speed $n^* = 2500rpm$. Then at $t = 1.5sec$ a reverse speed is applied. The results are shown in Fig. 8.

The waveforms depicted in Fig. 7 show that the ideal field-oriented control is established by setting the flux responses $\psi_{dr} = 1Wb$, $\psi_{qr} = 0Wb$, despite the load variations. The step changes in the load torque and the reverse of speed response cause step change in the torque response without any effects on the fluxes responses, which are maintained constant, due to the decoupled control system between the torque and the rotor flux. Thus, the aim of the field-oriented control is achieved, and the introduction of perturbations is immediately rejected by the control system.

The aim of the third test is to solve the problem of detuning in indirect field-oriented control system in the case of parameter variations of the motor. The coefficients in equations systems (28)-(33) are all dependent on the motor parameters. These parameters may vary during on-line operation due to temperature or saturation effects. So, it is important to investigate the sensitivity of the complete system to parameters changes.

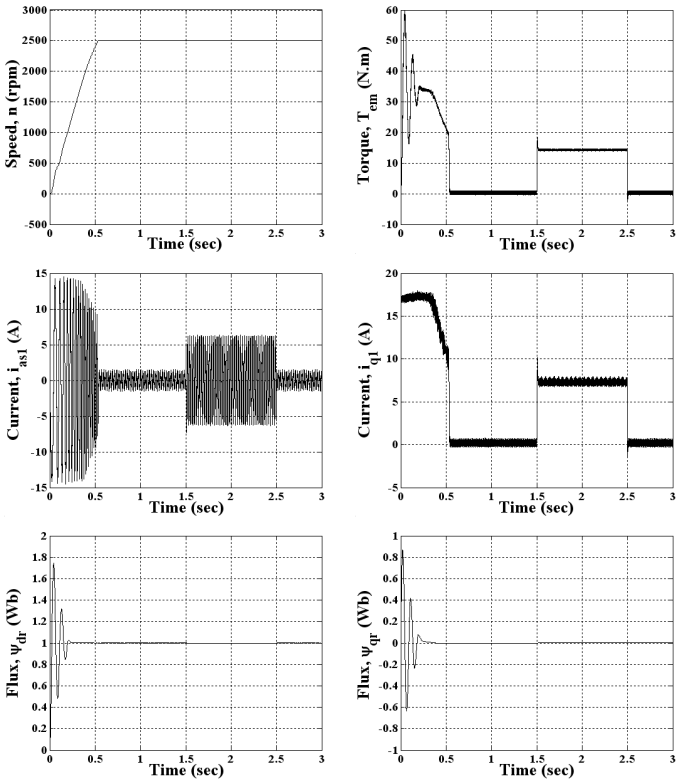

Fig. 7. Simulation results for a cascade structure using SMCs.

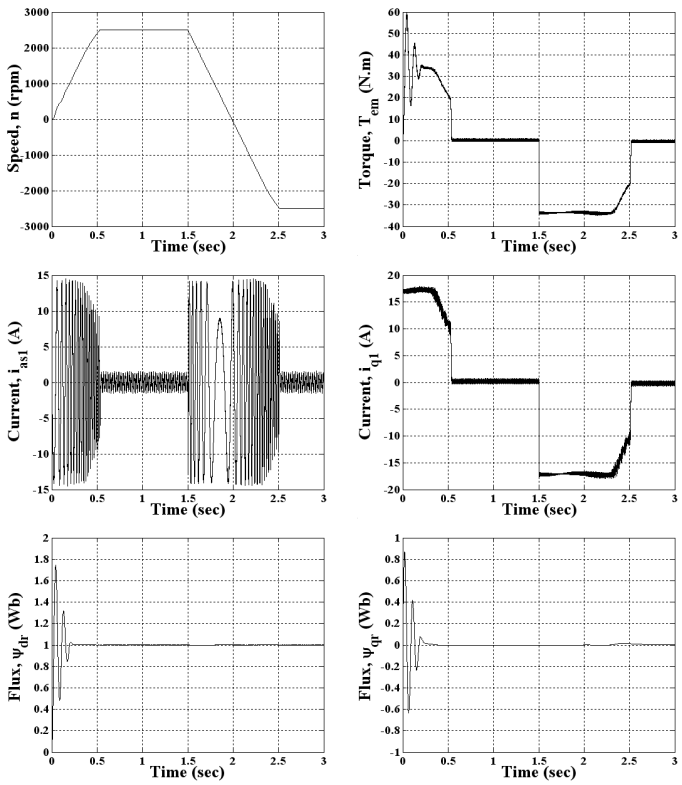

Fig. 8. Simulation results for a cascade structure using SMCs, with reverse speed at $t = 1.5sec$.

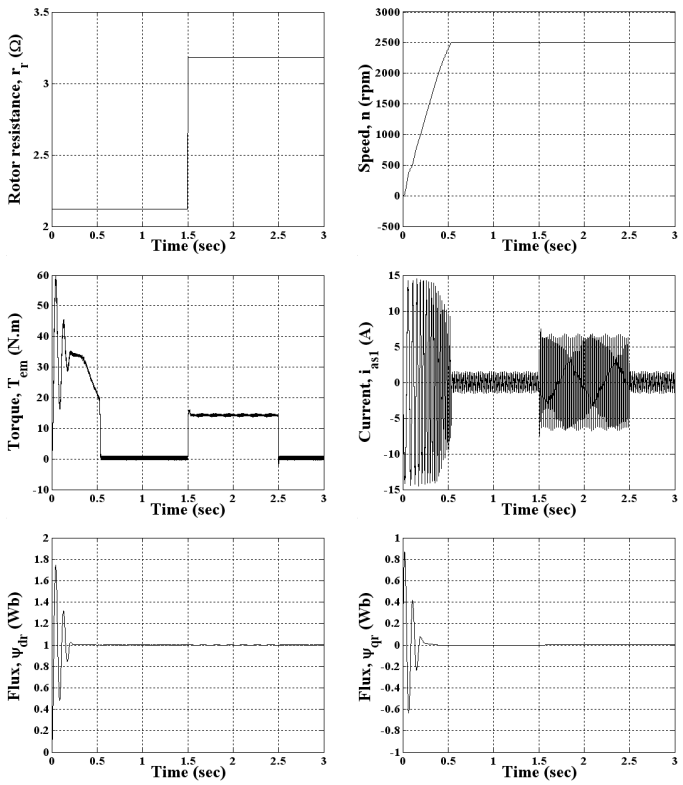

Fig. 9. Simulation results with variation 50% of r_r for an indirect FOC drive with SMCs.

One of the most significant parameter changes in the motor is the rotor resistance r_r. A simulation taking into account the variation of 50% rise of r_r relative to the identified model parameter was carried out. The parameters changes are introduced only in the model of the motor. Neither the estimator, nor the controller is involved by this variation. The waveforms obtained are illustrated in Fig. 9. The responses are approximately similar to chose obtained in Fig. 7 and the condition of oriented control is obtained in the steady state ($\psi_{qr} = 0Wb$). Therefore, the sliding mode controller can ensure a correct robustness against uncertainties of parameters of the motor. In practice, this fact is important because it is impossible to have an exact value of each parameter of the machine.

VIII. Conclusion

A sliding mode control for dual-stator induction motor drives fed by matrix converters has been presented in this paper. The first part is dedicated to the description of the DSIM and the mathematical model and the field oriented control of a DSIM. In the second part, the sliding mode control strategy is presented and applied to control of the DSIM. In the third part, matrix converter modeling is presented.

Simulation results have been carried out, validating, the effectiveness of the proposed controllers and successfully implemented a dual-stator induction motor drives.

Appendix

The machine parameters used in the simulation are as follows:

- Nominal voltage: $v_n = 220V$;
- Nominal current: $\imath_n = 6.5A$;
- Stator resistances per phase (winding set I and II) $r_1 = r_2 = 3.72\Omega$;
- Stator self inductances per phase (winding set I and II) $L_1 = L_2 = 0.022H$;
- Rotor resistance per phase $r_r = 2.12\Omega$;
- Rotor self inductance per phase $L_r = 0.006H$;
- Mutual inductance between stator and rotor $L_m = 0.3672H$;
- Inertia $J = 0.0625kg.m^2$;
- Viscous friction $f = 0.001N.m.s/rd$;
- Number of pole pairs $P = 1$.

References

[1] P. L. Alger and R. E. Arnold, "The history of induction motors in America," *in Proc. IEEE*, vol. 64, no. 9, Sep. 1976, pp. 1380–1383.

[2] Y. Zhao and T. A. Lipo, "Space vector PWM control of dual three-phase induction machine using vector space decomposition," *IEEE Trans. Ind. Appl.*, vol. 31, no. 5, pp. 1100–1109, Sep./Oct. 1995.

[3] D. Hadiouche, H. Razik and A. Rezzoug, "On the modeling and design of dual-stator windings to minimize circulating harmonic currents for VSI fed AC machines," *IEEE Trans. Ind. Appl.*, vol. 40, no. 2, pp. 506–515, Mar./Apr. 2004.

[4] R. Bojoi, A. Tenconi, G. Griva and F. Profumo, "Vector control of dual-three-phase induction-motor drives two current sensors," *IEEE Trans. Ind. Appl.*, vol. 42, no. 5, pp. 1284–1292, Sep./Oct. 2006.

[5] E. A. Klingshirn, "High phase order induction motors-part I-description and theoretical considerations," *IEEE Trans. Power App. Syst.*, vol. PAS–102, no. 1, pp. 47–53, Jan. 1983.

[6] E. Levi, "Recent developments in high performance variable speed multiphase induction motor drives," *in Sixth Int. Symposium Nikola Tesla*, Belgrade, SASA, Serbia, Oct. 18–20, 2006.

[7] A. Djahbar, B. Mazari and M. Latroch, "Control strategy of three-phase matrix converter fed induction motor drive system," *IEE Power Conversion Appl. Professional Network*, Printed and published by the IEE, Michael Faraday House, Six Hills Way, Stevenage, Herts SG1 2AY, UK, pp. 11/1–11/6.

[8] K. Lee and F. Blaabjerg, "A nonlinearity compensation method for a matrix converter drive," *IEEE Power Electron. Letters*, vol. 3, no. 1, pp. 19–23, Mar. 2005.

[9] K. Ghedamsi, D. Aouzellag and E. M. Berkouk, "Control of wind generator associated to a flywheel energy storage system," *ScienceDirect*, Elsevier, Renewable Energy 33, pp. 2145–2156, 2008.

[10] K. Lee and F. Blaabjerg, "Improved sensorless vector control for induction motor drives fed by a matrix converter using nonlinear modeling and disturbance observer," *IEEE Trans. Energy Convers.*, vol. 21, no. 1, pp. 52–59, Mar. 2006.

[11] K. Ghedamsi, "Contribution to modeling and control to the direct frequency converter and its application to drive the doubly fed induction generator," (in french), Ph.D. dissertation, Ecole nationale polytechnique, ENP, Alger, Algeria, Dec. 2008.

[12] M. Venturini, "The generalized transformer: a new bidirectional sinusoidal waveform, frequency converter with continuously adjustable input power factor," *In Proc. PESC*, pp. 242–252, 1980.

[13] A. Alesina and M. Venturini, "Intrinsic amplitude limits and optimum design of 9 switches direct PWM ac-ac converter," *In Proc. PESC Conf.*, pp. 1284-1290, Rec. Apr. 1988.

[14] V. I. Utkin, "Variable structure systems with sliding modes," *IEEE Trans. Autom. Control*, vol. AC–22, no. 2, pp. 212–222, Apr. 1977.

[15] S. J. Huang and H. Y. Chen, "Adaptive sliding controller with self-tuning fuzzy compensation for vehicle suspension control," *ScienceDirect*, Elsevier, Mechatronics 16, pp. 607–622, 2006.

[16] J.-J. E. Slotine and W. Li "Applied nonlinear control," Englewood Cliffs, New Jersey, Prentice–Hall, 1991.

[17] M. Abid, A. Mansouri, A. G. Aissaoui and B. Belabbes, "Sliding mode application in position control of an induction machine," *Journal Elec. Engineering, JEEEC*, vol. 59, no. 6, pp. 322–327, 2008.

[18] K. D. Young, V. I. Utkin and Ü. Özgüner, "A control engineer's guide to sliding mode control," *IEEE Control Syst. Technology*, vol. 7, no. 3, pp. 328–342, May 1999.

[19] A. G. Loukianov, J. M. Cañedo, V. I. Utkin and J. C. Vázquez, "Discontinuous controller for power systems: sliding-mode block control approach," *IEEE Trans. Ind. Electron.*, vol. 51, no. 2, pp. 340–353, Apr. 2004.

[20] D. Hadiouche, "Contribution to the study of dual stator induction machines: Modeling, supplying and structure," (in french), Ph.D. dissertation, GREEN, Faculty Sci. Tech. Univ. Henri Poincar-Nancy I, Vandoeuvre-lès-Nancy, France, Dec. 2001.

[21] H. Amimeur, R. Abdessemed, D. Aouzellag, E. Merabet and F. Hamoudi, "Modeling and Analysis of Dual-Stator Windings Self-Excited Induction Generator," *Journal Elec. Engineering JEE*, art. 3, iss. 3, vol. 8, 2008.

[22] G. K. Singh, K. Nam and S. K. Lim, "A simple indirect field-oriented control scheme for multiphase induction machine," *IEEE Trans. Ind. Electron.*, vol. 52, no. 4, pp. 1177–1184, Aug. 2005.

[23] D. Berbier, E. M. Berkouk, A. Talha and M. O. Mahmoudi, "Study and control of two-level PWM rectifiers-clamping bridge-two three-level NPC VSI cascade. Application to double stator induction machine," *in 35th Annual IEEE Power Electron. Specialists Conf.*, Aachen, Germany, 2004, pp. 3894–3899.

[24] Z. Oudjebour, E. M. Berkouk, N. Sami, S. Belgasmi, S. Arezki and I. Messaif, "Indirect space vector control of a double star induction machine fed by two five-levels NPC VSI," *in Int. Conf. Elec. Mach.*, ICEM'04, Poland, 2004.

[25] H. Amimeur, R. Abdessemed, D. Aouzellag, E. Merabet and F. Hamoudi, "A sliding mode control associated to the field-oriented control of dual-stator induction motor drives," *Journal Elec. Engineering JEE*, art. 2, iss. 3, vol. 10, 2010.

[26] A. Hazzab, I. K. Bousserhane and M. Kamli, "Design of a fuzzy sliding mode controller by genetic algorithms for induction machine speed control," *Int. Journal Emerging Elec. Power Syst.*, vol. 1, iss. 2, art. 1008, pp. 1–17, 2004.

[27] M. F. Benkhoris and A. Gayed, "Discrete sliding control technique of DC motor drive," *in IEE Conf. publication Power Electron. Variable Speed drives*, no. 429, Sep. 23–25, 1996, pp. 81–86.

[28] HJ. Cha, "Analysis and design of matrix converter for adjustable speed drives and distributed power sources," Ph.D. Thesis, Texas A&M University, Aug. 2004.